

Noise-induced perturbations of dispersion-managed solitons

Jinglai Li, Elaine Spiller, and Gino Biondini

Department of Mathematics, State University of New York at Buffalo, Buffalo, New York 14260, USA

(Received 9 January 2007; published 18 May 2007)

We study noise-induced perturbations of dispersion-managed solitons. We do so by first developing soliton perturbation theory for the dispersion-managed nonlinear Schrödinger (DMNLS) equation, which governs the long-term behavior of optical fiber transmission systems and certain kinds of femtosecond lasers. We show that the eigenmodes and generalized eigenmodes of the linearized DMNLS equation around traveling-wave solutions can be generated from the invariances of the DMNLS equations, we quantify the perturbation-induced parameter changes of the solution in terms of the eigenmodes and the adjoint eigenmodes, and we obtain evolution equations for the solution parameters. We then apply these results to guide importance-sampled Monte Carlo (MC) simulations and reconstruct the probability density functions of the solution parameters under the effect of noise, and we compare with standard MC simulations of the unaveraged system. The comparison further validates the use of the DMNLS equation as a model for dispersion-managed systems.

DOI: [10.1103/PhysRevA.75.053818](https://doi.org/10.1103/PhysRevA.75.053818)

PACS number(s): 42.65.Tg, 02.70.Uu, 42.65.Sf

I. INTRODUCTION

Dispersion management has become an essential component not only of modern optical fiber communication systems [1,2], but also of certain femtosecond lasers [3]. The performance of both kinds of systems is affected by noise, which is an essential source of system failures. Because these systems are designed to operate with extremely high accuracies (typical values are one error per 10^{12} bits in communications and 1 part in 10^{18} for lasers used in optical atomic clocks), calculating failure rates analytically is extremely difficult since failures result from the occurrence of unusually large (and therefore atypical) deviations. At the same time, direct Monte Carlo computations of failure rates are impractical due to the exceedingly large number of samples that would be necessary to obtain a reliable estimate.

The effect of noise on optical transmission systems modeled by the nonlinear Schrödinger (NLS) equation has recently been studied [4–8] using a variance reduction technique called importance sampling (IS). In brief, IS biases the Monte Carlo simulations in such a way as to artificially increase the probability of achieving the rare events of interest, while correcting for the bias using appropriate likelihood ratios (e.g., see Refs. [9,10]). Use of IS makes it possible to efficiently estimate extremely small probabilities.

The key in successfully applying importance sampling lies in biasing towards the most likely noise realizations that lead to system failures. In the above-cited works, this was achieved by taking advantage of well-known results about the behavior of solutions of the NLS equation linearized around a soliton. This knowledge is not available, however, in systems with dispersion management. The aim of this work is to address this problem. We do so by employing the dispersion-managed NLS (DMNLS) equation which governs the long-term dynamics of dispersion-managed optical systems [11–13].

The layout of this paper is as follows. In Sec. II we develop a perturbation theory for dispersion-managed systems. First we study the connection between the invariances of DMNLS equation and solutions of the linearized DMNLS

equation. We then show how the equation invariances are connected to the existence of traveling-wave solutions. We also show that the linearized DMNLS around such traveling-wave solutions can be expressed in terms of an integro-differential operator whose eigenmodes and generalized eigenmodes can also be generated from the invariances. Finally, we use these linear modes and their adjoints to quantify the perturbation-induced parameter changes, using the relation between the linear modes and the derivatives of the solution with respect to the invariance parameters. In Sec. III we use these theoretical results to guide importance-sampled Monte Carlo simulations of noise-induced perturbations in dispersion-managed lightwave systems and reconstruct the probability density functions of the output solution parameters.

II. SYMMETRIES AND PERTURBATIONS OF DISPERSION-MANAGED SYSTEMS

It is well known that the propagation of coherent optical pulses in dispersion-managed systems can be described by the following perturbed NLS equation:

$$i\frac{\partial u}{\partial t} + \frac{1}{2}d(t/t_a)\frac{\partial^2 u}{\partial x^2} + g(t/t_a)|u|^2u = 0. \quad (2.1)$$

Here all quantities are in dimensionless units; t is the propagation distance, x is the retarded time (that is, the time in a reference frame that moves with the group velocity of the pulse), and $u(x, t)$ is the slowly varying envelope of the optical field, rescaled (if necessary in communications) to take into account periodic loss and amplification. The function $d(t/t_a)$ represents the local dispersion, while $g(t/t_a)$ describes the periodic power variation due to loss and amplification. [That is, the optical amplitude is proportional to $\sqrt{g(t/t_a)}u(x, t)$.] Both $d(\cdot)$ and $g(\cdot)$ are taken to be periodic with unit period. The particular choice of $d(t/t_a)$ is called a dispersion map, and the quantity t_a is called the dispersion map period. Systems described by Eq. (2.1) include modern optical fiber communication systems [1,2] as well as certain femtosecond lasers [3].

A. The DMNLS equation, invariances, and soliton solutions

Some of the invariances of the “pure” NLS equation [namely, Eq. (2.1) with $d(\cdot)=g(\cdot)=1$] are lost with dispersion management. (More precisely, time translations, scaling and Galilean invariance are broken, although a generalized Galilean invariance exists.) Moreover, Eq. (2.1) is a nonlinear partial differential equation (PDE) with nonconstant coefficients which contain large and rapid variations; the asymptotic behavior of its solutions is therefore not apparent. As shown in Ref. [11], an appropriate multiple-scale analysis of Eq. (2.1) shows that, once the periodic compression-expansion breathing of the pulse is properly factored out, the core pulse shape obeys a nonlinear, nonlocal equation of nonlinear-Schrödinger type called the dispersion-managed NLS (DMNLS) equation [13]. Without repeating the derivation here, we note that the key is to split the dispersion $d(t/t_a)$ into the sum of two components: A mean value \bar{d} and a term describing the large, zero-mean rapid variations corresponding to the large local values of dispersion:

$$d(t/t_a) = \bar{d} + \frac{1}{t_a} \Delta D(t/t_a). \quad (2.2)$$

To leading order, the solution of Eq. (2.1) is then

$$\hat{u}(\omega, t, \zeta) = \hat{u}'(\omega, t) e^{-iC(\zeta)\omega^2/2}, \quad (2.3)$$

where $\zeta = t/t_a$ and

$$C(\zeta) = C_0 + \int_0^\zeta \Delta D(\zeta') d\zeta', \quad (2.4)$$

with C_0 an arbitrary integration constant. Above and hereafter, $\hat{f}(\omega) = \mathcal{F}_\omega[f(x)] = \int e^{-i\omega x} f(x) dx$ is the Fourier transform of $f(x)$. The exponential factor in Eq. (2.3) accounts for the rapid breathing of the pulse, while the slowly varying envelope $\hat{u}'(\omega, t)$ satisfies the DMNLS equation, which in the physical and Fourier domains, is respectively (omitting primes for simplicity)

$$i \frac{\partial u}{\partial t} + \frac{1}{2} \bar{d} \frac{\partial^2 u}{\partial x^2} + \iint u_{(x+x')} u_{(x+x'')} u_{(x+x'+x'')}^* R_{(x',x'')} dx' dx'' = 0, \quad (2.5a)$$

$$i \frac{\partial \hat{u}}{\partial t} - \frac{1}{2} \bar{d} \omega^2 \hat{u} + \iint \hat{u}_{(\omega+\omega')} \hat{u}_{(\omega+\omega'')} \hat{u}_{(\omega+\omega'+\omega'')}^* r_{(\omega',\omega'')} d\omega' d\omega'' = 0, \quad (2.5b)$$

where the asterisk denotes complex conjugation and where for brevity we introduced the shorthand notations $u_{(x)} = u(x, t)$, $\hat{u}_{(\omega)} = \hat{u}(\omega, t)$, etc. Throughout this work, integrals are complete unless limits are explicitly stated. The integration kernels $r(y)$ and $R(x', x'')$ in Eqs. (2.5a) and (2.5b) quantify the average nonlinearity over a dispersion map mitigated by the dispersion management, and are given respectively by

$$r(y) = \frac{1}{(2\pi)^2} \int_0^1 g(\zeta) e^{iC(\zeta)y} d\zeta, \quad (2.6a)$$

$$R(x', x'') = \frac{1}{2\pi} \iint e^{-i\omega'x' - i\omega''x''} r(\omega', \omega'') d\omega' d\omega''. \quad (2.6b)$$

Note that both focusing and defocusing cases can be obtained in Eqs. (2.5a) and (2.5b) depending on the sign of the average dispersion \bar{d} .

It is crucial to realize that the DMNLS equation and its solutions depend implicitly on a parameter, called the dimensionless *reduced map strength*, which quantifies the size of the zero-mean dispersion fluctuations. The map strength s can be defined for any dispersion map as

$$s = \frac{1}{4} \|\Delta D\|_1 = \frac{1}{4} \int_0^1 |\Delta D(\zeta)| d\zeta. \quad (2.7)$$

One can then formally obtain the dependence of the kernels $r(y)$ and $R(x', x'')$ on the map strength by writing $\Delta D(\zeta)$ and $C(\zeta)$ in terms of normalized functions which only depend on the shape of the zero-mean dispersion variations. Namely, one writes $\Delta D(\zeta) = 4s \Delta D_1(\zeta)$ and $C(\tau) = 4s C_1(\tau)$, where $C_1(\zeta)$ is given by Eq. (2.4) with $\Delta D(\zeta)$ replaced by $\Delta D_1(\zeta)$. In this way, one can conveniently study cases with different map strengths entirely within the framework of the DMNLS equation, without needing to refer to Eq. (2.1). Of course, in the limit $s \rightarrow 0$, one obtains $r(y) \rightarrow 1/(2\pi)^2$ and $R(x', x'') \rightarrow \delta(x') \delta(x'')$. That is, as $s \rightarrow 0$ the DMNLS equation (2.5a) reduces to the pure NLS equation.

The DMNLS equation (2.5a) is a reduced model that retains the essential features of dispersion-managed systems while bypassing the complicated dynamics that take place within each dispersion map. As such, it has proved to be a useful model to investigate the long-time behavior of dispersion-managed systems [11–28]

In the case where loss and gain are perfectly balanced (e.g., with distributed Raman amplification in communication systems [29]) it is $g(\cdot)=1$, and both kernels can then be made real by proper choice of the integration constants. Here we assume that this has been done. Then, in the special but physically important case of a piecewise constant, two-step dispersion map, the kernels assume a particularly simple form [11]:

$$r(y) = \frac{1}{(2\pi)^2} \frac{\sin sy}{sy}, \quad R(x', x'') = \frac{1}{2\pi|s|} \text{ci}(x'x''/s), \quad (2.8)$$

where $\text{ci}(x) = \int_1^\infty \cos(xy)/y dy$. Note that, in this case, both kernels are independent of the particular shape of the zero-mean dispersion variations. The same kernels, apart from a factor 2, also arise for the DMNLS equation as a model of certain femtosecond lasers [12].

Stationary solutions of the DMNLS equation are obtained by looking for solutions of the form

$$u_{st}(x, t; s) = e^{i\lambda^2 t/2} f(x; s). \quad (2.9)$$

The Fourier transform $\hat{f}(\omega)$ of $f(x)$ then solves the nonlinear integral equation [11]

$$(\lambda^2 + \bar{d}\omega^2)\hat{f}_{(\omega)} = 2 \int \int \hat{f}_{(\omega+\omega')} \hat{f}_{(\omega+\omega'')} \hat{f}_{(\omega+\omega'+\omega'')}^* r_{(\omega',\omega'')} d\omega' d\omega'', \quad (2.10)$$

which can be efficiently computed numerically (cf. Appendix 2). Note that, like in the NLS equation, the “soliton eigenvalue” λ is also the peak amplitude of the pulse, independent of map strength.

Remarkably, some of the invariances of the standard NLS equation that are destroyed by dispersion management are recovered by the DMNLS equation. In particular, the following NLS invariances also hold for the DMNLS equation without modification: phase invariance, position invariance, time invariance, and Galilean invariance, which are respectively

$$u \rightarrow e^{i\phi_0} u, \quad (2.11a)$$

$$x \rightarrow x - x_0, \quad (2.11b)$$

$$t \rightarrow t - t_0, \quad (2.11c)$$

$$x \rightarrow x - \Omega t, \quad u \rightarrow e^{i\Omega x - i\Omega^2 t/2} u. \quad (2.11d)$$

On the other hand, unlike the NLS equation, the DMNLS equation is not scale invariant. Rather, the DMNLS equation admits a generalized scaling invariance which also involves the map strength:

$$x \rightarrow x/A, \quad t \rightarrow t/A^2, \quad s \rightarrow s/A^2, \quad u \rightarrow Au. \quad (2.11e)$$

Starting from Eq. (2.9), a four-parameter family of traveling-wave solutions can then be generated by using the invariances (2.11a), (2.11b), (2.11c), (2.11d), and (2.11e):

$$u(x,t) = A e^{i[\Omega x + (1/2)(A^2 - \Omega^2)t + \phi_0]} f(A(x - x_0 - \Omega t); A^2 s), \quad (2.12a)$$

or, equivalently,

$$u(x,t) = A e^{i(\Omega x + \Phi)} f(A(x - X); A^2 s), \quad (2.12b)$$

where

$$X(t) = x_0 + \Omega t, \quad \Phi(t) = (A^2 - \Omega^2)t/2 + \phi_0 \quad (2.13)$$

are respectively the mean position and an overall phase. Note that for the stationary solution (2.9), time translations can be expressed as a composition of phase transformations and position translations. Hence, even though five invariances exist, there are only four independent solution parameters for traveling-wave solutions. When the kernel $r(y)$ is real, $f(x)$ can be taken to be real and even. Solutions (2.12a) are usually referred to as dispersion-managed solitons (DMS).

B. Linear modes of the DMNLS equation

We now consider the stability of solutions under perturbations. If $u(x,t)$ is any solution of the DMNLS equation and $u(x,t) + \epsilon v(x,t)$ is also a solution, $v(x,t)$ solves the linearized

DMNLS equation around $u(x,t)$; namely, $L[v,u]=0$, where [21,25]

$$\begin{aligned} L[v,u] = & \frac{\partial v}{\partial t} - \frac{i}{2} \bar{d} \frac{\partial^2 v}{\partial x^2} \\ & - 2i \int \int u_{(x+x')} u_{(x+x'')}^* v_{(x+x')} R_{(x',x'')} dx' dx'' \\ & - i \int \int u_{(x+x')} u_{(x+x'')}^* v_{(x+x'')} R_{(x',x'')} dx' dx'' \end{aligned} \quad (2.14)$$

is the linearized DMNLS operator. Since the DMNLS equation is not integrable [15,20], its linear modes cannot be derived from the inverse scattering method as for the NLS equation [30]. The linear modes, however, can be generated using the invariances (2.11a), (2.11b), (2.11c), (2.11d), and (2.11e). Suppose that $u(x,t)$ solves some PDE, and consider a generic infinitesimal transformation $u(x,t) \rightarrow u_\epsilon(x,t)$, with

$$u_\epsilon(x,t) = u(x,t) + \epsilon v(x,t) + O(\epsilon^2), \quad (2.15a)$$

and

$$v(x,t) = \left. \frac{\partial u_\epsilon(x,t)}{\partial \epsilon} \right|_{\epsilon=0}. \quad (2.15b)$$

If the PDE is invariant under the above transformation, one verifies that $v(x,t)$ is in the nullspace of $L[\cdot, u]$; namely, $v(x,t)$ is a solution of the linearized PDE about the given solution. When applied to the DMNLS equation, this construction yields four solutions of the linearized DMNLS equation around any solution $u(x,t)$. More precisely, these solutions of the linearized DMNLS equation, which are associated with the phase, distance translation, Galilean invariance, and scale invariance, are, respectively,

$$v_1 = iu, \quad v_2 = -\frac{\partial u}{\partial x}, \quad (2.16a)$$

$$v_3 = iXu - t \frac{\partial u}{\partial x}, \quad v_4 = u + x \frac{\partial u}{\partial x} + 2t \frac{\partial u}{\partial t} + 2s \frac{\partial u}{\partial s}. \quad (2.16b)$$

Note that v_3 and v_4 are not bounded in time. Using the fact that $L[v,u]=w$ implies $L[tv,u]=tw+v$, however, one can convert v_3 and v_4 into bounded elements of the generalized null space of L . Note also that a further solution of the linearized DMNLS equation, namely $v_5 = -u_t$, can be generated from invariance with respect to time translations. This fifth solution of the linearized equation, however, is *not* linearly independent from the other four if $u(x,t)$ is the traveling-wave solution (2.12a), since then

$$v_5 = \frac{1}{2}(A^2 + \Omega^2)v_1 + \Omega v_2. \quad (2.17)$$

For traveling-wave solutions, it is possible to express the linearized DMNLS equation in terms of an ordinary differential operator by performing a change of coordinates to the

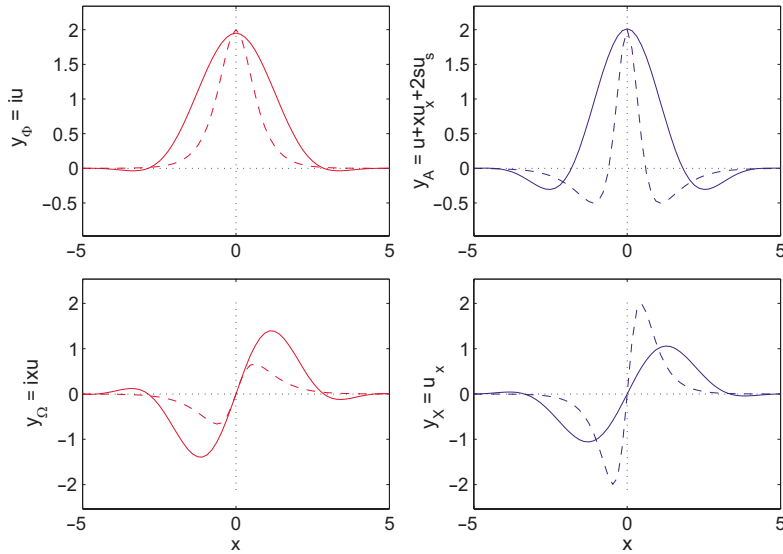


FIG. 1. (Color online) The shape of the neutral eigenmodes and generalized eigenmodes of the DMNLS equation for $s=2$ (solid lines), compared to the corresponding modes for the NLS equation ($s=0$, dashed lines), with $\bar{d}=1$ and $A=2$ in both cases. Top left: phase mode; top right: amplitude mode; bottom left: frequency mode; bottom right: position mode. Blue lines (top right and bottom right plots) show components in phase with the pulse; red lines (top left and bottom left plots) show components 90° out of phase.

comoving frame (ξ, t') , with $\xi=x-X(t)$ and $t'=t$, and writing $u(x, t)$ and $v(x, t)$ respectively as

$$u(x, t) = e^{i\Theta} U(\xi), \quad v(x, t) = e^{i\Theta} y(\xi, t'), \quad (2.18)$$

where $\Theta(x, t) = \Omega x + \Phi(t)$ is the local phase and $U(\xi) = Af(A\xi)$ the pulse envelope. Substituting Eq. (2.18) into Eq. (2.14) yields

$$e^{-i\Theta} L[v; u] = \frac{\partial y}{\partial t'} - \Lambda[y; U], \quad (2.19)$$

where

$$\begin{aligned} \Lambda[y, U] = & \frac{i}{2} \bar{d} \frac{\partial^2 y}{\partial \xi^2} - \frac{i}{2} A^2 y \\ & + 2i \int \int U_{(\xi+\xi')} U_{(\xi+\xi'+\xi'')}^* y_{(\xi+\xi')} R_{(\xi', \xi'')} d\xi' d\xi'' \\ & + i \int \int U_{(\xi+\xi')} U_{(\xi+\xi'')}^* y_{(\xi+\xi'+\xi'')} R_{(\xi', \xi'')} d\xi' d\xi''. \end{aligned} \quad (2.20)$$

Since a zero eigenvalue implies neutral stability, we will call y a neutral eigenmode if $\Lambda[y, U]=0$ and a generalized eigenmode if $\Lambda[y, U]$ is a neutral eigenmode [25]. Using Eqs. (2.18) and (2.19), one can associate each solution of the linearized DMNLS in Eqs. (2.16a) and (2.16b) to a neutral eigenmode or generalized eigenmode of $\Lambda[y, U]$. After rearranging terms, one can obtain the following set of modes and generalized modes:

$$y_\Phi = iU, \quad y_X = -\frac{\partial U}{\partial \xi}, \quad (2.21a)$$

$$y_\Omega = i\xi U, \quad y_A = \frac{1}{A} \left(U + \xi \frac{\partial U}{\partial \xi} + 2s \frac{\partial U}{\partial s} \right) \quad (2.21b)$$

(where the subscript associates each mode to the solution parameters changed by the transformation), which satisfy the following relations:

$$\Lambda[y_\Phi, U] = 0, \quad \Lambda[y_X, U] = 0, \quad (2.22a)$$

$$\Lambda[y_\Omega, U] = y_X, \quad \Lambda[y_A, U] = Ay_\Phi. \quad (2.22b)$$

Note the explicit dependence on s of the amplitude mode y_A , as well as, of course, of the corresponding solution of the linearized DMNLS equation, v_4 . Note also that, as for the NLS equation, some freedom exists in the definition of the generalized modes, as well as in the normalization of all modes. Importantly, for $Q=A, X, \Phi$ it is

$$\frac{\partial u}{\partial Q} = e^{i\Theta} y_Q, \quad (2.23a)$$

while

$$\frac{\partial u}{\partial \Omega} = e^{i\Theta} (y_\Omega + Xy_\Phi). \quad (2.23b)$$

Of course, different parametrization of the traveling-wave solution will also result in different combinations of modes. The shape of the modes in Eqs. (2.21a) and (2.21b) is shown in Fig. 1 for $s=0$ (NLS) and $s=2$.

In order to quantify the effect of perturbations, it is necessary to also employ the adjoint modes. Introducing the inner product as

$$\langle y, w \rangle = \text{Re} \int y^*(x) w(x) dx = \int (y_{\text{Re}} w_{\text{Re}} + y_{\text{Im}} w_{\text{Im}}) dx, \quad (2.24)$$

the adjoint of $\Lambda[y, U]$ is found to be

$$\begin{aligned} \Lambda^\dagger[y, U] = & -\frac{i}{2} \bar{d} \frac{\partial^2 y}{\partial \xi^2} + \frac{i}{2} A^2 y \\ & - 2i \int \int U_{(\xi+\xi')} U_{(\xi+\xi'+\xi'')}^* y_{(\xi+\xi')} R_{(\xi', \xi'')} d\xi' d\xi'' \\ & + i \int \int U_{(\xi+\xi')} U_{(\xi+\xi'')}^* y_{(\xi+\xi'+\xi'')} R_{(\xi', \xi'')} d\xi' d\xi''. \end{aligned} \quad (2.25)$$

Note that $\Lambda^\dagger[y, U] = -i\Lambda[iy, U]$. Using this property, one can immediately obtain the adjoint modes of Eqs. (2.21a) and (2.21b), i.e., the eigenmodes of $\Lambda^\dagger[y, U]$:

$$\underline{y}_\Phi = \frac{i}{A} \left(U + \xi \frac{\partial U}{\partial \xi} + 2s \frac{\partial U}{\partial s} \right), \quad \underline{y}_X = \frac{1}{A} \xi U, \quad (2.26a)$$

$$\underline{y}_\Omega = -\frac{i}{A} \frac{\partial U}{\partial \xi}, \quad \underline{y}_A = U, \quad (2.26b)$$

satisfying relations analogous to Eqs. (2.22a) and (2.22b) (Note, however, that $\underline{y}_Q \neq \pm iy_Q$, and the adjoint of a neutral eigenmode is a generalized eigenmode, and vice versa.) Due to the real and even nature of $f(x)$, the modes (2.21a) and (2.21b) and their adjoints (2.26a) and (2.26b) form a biorthogonal set which provides a basis of the generalized null space of Λ . Explicitly,

$$\langle \underline{y}_Q, \underline{y}_{Q'} \rangle = \langle \underline{y}_Q, \underline{y}_{Q'} \rangle \delta_{QQ'}, \quad (2.27)$$

where

$$\langle \underline{y}_A, \underline{y}_A \rangle = \langle \underline{y}_\Phi, \underline{y}_\Phi \rangle = \left(\frac{1}{2} + 2s \frac{\partial}{\partial s} \right) E/A, \quad (2.28a)$$

$$\langle \underline{y}_X, \underline{y}_X \rangle = \langle \underline{y}_\Omega, \underline{y}_\Omega \rangle = \frac{1}{2} E/A, \quad (2.28b)$$

and where $E = \|u\|^2 = \int |u(x, t)|^2 dx$ is the pulse energy. Note that, unlike the case of the NLS equation, these adjoint modes are not normalized, and in general the norms $\|\underline{y}_Q\|^2 = \langle \underline{y}_Q, \underline{y}_Q \rangle$ depend on both s and λ , as shown in Fig. 2. Note how the inner products become progressively larger with increasing map strength. Of course the orthonormality could be achieved by properly redefining the adjoint modes, but the present choice is convenient for our purposes. For the NLS equation it is simply $s=0$ and $E=2A$, so in that case the modes are indeed biorthogonal. As we show next, these linear modes and adjoint modes can be used to quantify perturbation-induced solution parameter changes.

C. Perturbation-induced parameter changes

We now consider perturbations which manifest as an additional term in the NLS equation (2.1):

$$i \frac{\partial u}{\partial t} + \frac{1}{2} d(t/t_a) \frac{\partial^2 u}{\partial x^2} + g(t/t_a) |u|^2 u = i \epsilon h(x, t), \quad (2.29)$$

with $0 < \epsilon \ll 1$. In Sec. III we will explicitly discuss the case in which $h(x, t)$ is a noise process. The above formulation, however, is of course very general, and it includes most physically interesting situations such as damping, amplification, third-order dispersion, shock and Raman effects (e.g., see Refs. [1,31]). Using the same multiple scale analysis as for Eq. (2.1), from Eq. (2.29) one obtains a perturbed DMNLS equation in which an inhomogeneous term is added to the right-hand side (RHS):

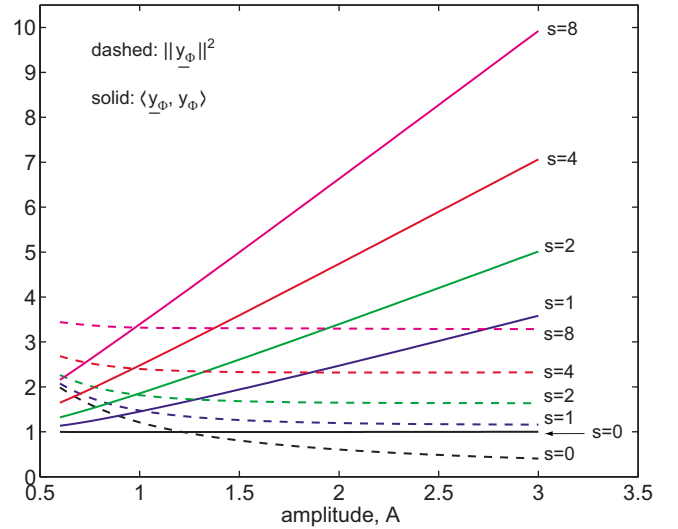
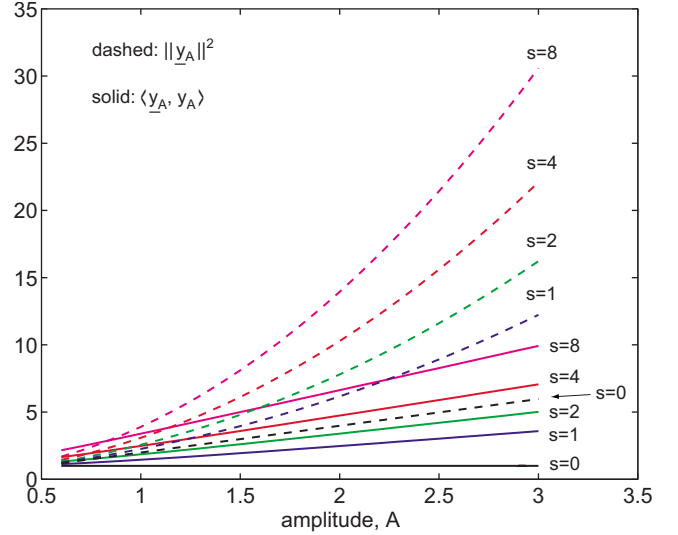


FIG. 2. (Color online) Top: L_2 norm of the amplitude mode \underline{y}_A and the inner product $\langle \underline{y}_A, \underline{y}_A \rangle$ as a function of the amplitude parameter A for different values of map strength. Bottom: L_2 norm of \underline{y}_Φ and the inner product $\langle \underline{y}_\Phi, \underline{y}_\Phi \rangle$ as a function of the amplitude parameter A .

$$i \frac{\partial u}{\partial t} + \frac{1}{2} d \frac{\partial^2 u}{\partial x^2} + \int \int u_{(x+x')} u_{(x+x'')} u_{(x+x'+x'')}^* R_{(x',x'')} dx' dx'' = i \epsilon h(x, t). \quad (2.30)$$

Now suppose $u_\epsilon = u + \epsilon v$ solves Eq. (2.30), where u is a traveling-wave solution of the unperturbed DMNLS equation given by Eq. (2.12a), and ϵv is the perturbation-induced solution change. Then the perturbation $v(x, t)$ satisfies the perturbed linearized DMNLS equation,

$$L[v, u] = h. \quad (2.31)$$

Of course, in order for the perturbation expansion to remain well-ordered, the solutions of Eq. (2.31) must remain bounded. If, however, the right-hand side of Eq. (2.31) has a nonzero component along the null space of L , secular terms will arise. As usual, such terms are removed by requiring that

the parameters of the unperturbed solution become slowly varying functions of time [32]. Namely, introducing the fast and slow time scales $t_1=t$ and $t_2=\epsilon t$, one obtains

$$\frac{\partial u}{\partial t} = \frac{\partial u}{\partial t_1} + \epsilon \sum_Q \frac{\partial u}{\partial Q} \frac{\partial Q}{\partial t_2}, \quad (2.32)$$

where now $Q=A, \Omega, X, \Phi$. The perturbed linearized DMNLS equation (2.31) therefore becomes

$$L_1[v, u] + \sum_Q \frac{\partial u}{\partial Q} \frac{\partial Q}{\partial t_2} = h, \quad (2.33)$$

where $L_1[v, u]$ is given by Eq. (2.14) with $\partial/\partial t$ replaced by $\partial/\partial t_1$. Recalling Eqs. (2.19) and (2.23a) and (2.23b), one can rewrite Eq. (2.33) as

$$\frac{\partial w}{\partial t_1} - \Lambda_1[w, U] + X y_\Phi \frac{\partial \Omega}{\partial t_2} + \sum_Q y_Q \frac{\partial Q}{\partial t_2} = e^{-i\Theta} h, \quad (2.34)$$

where $w(x, t) = e^{-i\Theta(x, t)} v(x, t)$ and where $\Lambda_1[w, U]$ is given by Eq. (2.20) with $t' = t_1$ and $\xi = x - X(t_1)$. [The extra term proportional to y_Φ comes from Eq. (2.23b).] We now decompose the right-hand side of Eq. (2.34a) as

$$h = \sum_Q \frac{\langle e^{i\Theta} \underline{y}_Q, h \rangle}{\langle \underline{y}_Q, \underline{y}_Q \rangle} e^{i\Theta} y_Q + h_{\text{res}}, \quad (2.35a)$$

so that

$$\langle e^{i\Theta} \underline{y}_Q, h_{\text{res}} \rangle = 0 \quad (2.35b)$$

for $Q=A, \Omega, X, \Phi$. The solvability condition (namely the requirement that the resulting PDE for w contain no secular terms) then provides evolution equations for the solution parameters:

$$\frac{dA}{dt} = \epsilon \frac{\langle e^{i\Theta} \underline{y}_A, h \rangle}{\langle \underline{y}_A, \underline{y}_A \rangle}, \quad (2.36a)$$

$$\frac{d\Omega}{dt} = \epsilon \frac{\langle e^{i\Theta} \underline{y}_\Omega, h \rangle}{\langle \underline{y}_\Omega, \underline{y}_\Omega \rangle}, \quad (2.36b)$$

$$\frac{dX}{dt} = \Omega + \epsilon \frac{\langle e^{i\Theta} \underline{y}_X, h \rangle}{\langle \underline{y}_X, \underline{y}_X \rangle}, \quad (2.36c)$$

$$\frac{d\Phi}{dt} = \frac{1}{2}(A^2 - \Omega^2) + \epsilon \frac{\langle e^{i\Theta} \underline{y}_\Phi, h \rangle}{\langle \underline{y}_\Phi, \underline{y}_\Phi \rangle} - \epsilon X \frac{\langle e^{i\Theta} \underline{y}_\Omega, h \rangle}{\langle \underline{y}_\Omega, \underline{y}_\Omega \rangle}. \quad (2.36d)$$

In the special case $h(x, t) = \Delta u(x) \delta(t - t_o)$, Eq. (2.30) describes changes in the initial condition. [Integrating from $t = t_o - \Delta t$ to $t = t_o + \Delta t$ and letting $\Delta t \rightarrow 0$ one has $u(x, t_o^+) = u(x, t_o^-) + \epsilon \Delta u(x)$.] In this case, Eqs. (2.36a), (2.36b), (2.36c), and (2.36d) yield the parameter changes as $Q(t_o^+) = Q(t_o^-) + \epsilon \Delta Q$, where

$$\Delta Q = \frac{\langle e^{i\Theta} \underline{y}_Q, \Delta u \rangle}{\langle \underline{y}_Q, \underline{y}_Q \rangle} \quad (2.37a)$$

for $Q=A, \Omega, X$, while

$$\Delta \Phi = \frac{\langle e^{i\Theta} \underline{y}_\Phi, \Delta u \rangle}{\langle \underline{y}_\Phi, \underline{y}_\Phi \rangle} - X \frac{\langle e^{i\Theta} \underline{y}_\Omega, \Delta u \rangle}{\langle \underline{y}_\Omega, \underline{y}_\Omega \rangle}. \quad (2.37b)$$

All of these results reduce to the standard perturbation theory for the NLS equation (e.g., see Refs. [5,31,33]) when $s=0$. The connection between invariances, conservation laws, and linear modes of the DMNLS equation is further explored in Ref. [18]. In Sec. III we will use the linear modes and Eqs. (2.37a) and (2.37b) to guide the simulations of noise-perturbed lightwave systems.

III. RARE EVENTS IN DISPERSION-MANAGED LIGHTWAVE SYSTEMS

As mentioned in the Introduction, the performance of both optical communication systems and certain femtosecond lasers is limited by noise. As a special but physically important example, we therefore now use the results of Sec. II to quantify the effects of noise on dispersion-managed solitons. Specifically, we take $h(x, t)$ in Eqs. (2.29) and (2.30) to be

$$h(x, t) = \sum_{n=1}^{N_a} v_n(x) \delta(t - nt_a), \quad (3.1)$$

where t_a is the dispersion map period, as before, and $\delta(t)$ is the Dirac delta distribution. In other words, $u(x, t)$ evolves according to the unperturbed DMNLS equation (2.5a) at all times except at $t = nt_a$, for $n = 1, \dots, N_a$, when

$$u(x, nt_a^+) = u(x, nt_a^-) + \epsilon v_n(x), \quad (3.2)$$

where $v_n(x)$ is taken to be normalized white Gaussian noise, satisfying

$$\mathbb{E}[v_n(x)] = 0, \quad \mathbb{E}[v_n(x) v_{n'}^*(x')] = \delta(x - x') \delta_{nn'}, \quad (3.3)$$

where $\mathbb{E}[\cdot]$ denotes ensemble average, and where in this case the small parameter ϵ^2 is the dimensionless noise variance. Starting from a soliton input pulse, namely $u(x, 0)$ given by Eq. (2.12), we are then interested in computing the probability density function (PDF) of the soliton parameters at the output time $N_a t_a$.

Even if the statistics of the noise sources are Gaussian, the resulting statistics at the output is not, in general, because propagation is nonlinear. Indeed, as mentioned earlier, the combination of noise and nonlinearity presents a formidable challenge if one is interested in calculating the probabilities of errors when performance standards dictate that errors be rare events. It has recently been shown that variance reduction methods such as importance sampling can be used to calculate PDFs in such systems accurate to very small probabilities [4–9]. Here we use the results of Sec. II to implement IS methods for the DMNLS equation in the presence of noise.

A. Importance sampling for the DMNLS equation

The idea behind importance sampling is straightforward: In order to calculate the probability of a desired rare event, sample the noise from a biased distribution that makes the rare events occur more frequently than would naturally be the case, while simultaneously correcting for the biasing.

Consider a set of random variables $\mathbf{X}=(x_1, \dots, x_N)$ distributed according to a joint probability distribution $p(\mathbf{X})$. The probability P that a function $y(\mathbf{X})$ falls into a desired range Y_d can be expressed via the multidimensional integral

$$P = \mathbb{P}[y \in Y_d] = \mathbb{E}[I(y(\mathbf{X}))] = \int I(y(\mathbf{x}))p(\mathbf{x})d\mathbf{x}, \quad (3.4a)$$

where the *indicator function* $I(y)$ equals 1 when $y \in Y_d$ and 0 otherwise. When exact evaluation of the integral is impossible (as it is in many practical cases due to the large dimensionality of sample space and the complicated form of the map from \mathbf{X} to y), one needs to resort to numerical methods. An unbiased estimator for P can be constructed via Monte Carlo (MC) quadrature as

$$\hat{P}_{\text{MC}} = \frac{1}{M} \sum_{m=1}^M I(y(\mathbf{X}_m)), \quad (3.4b)$$

where the M samples \mathbf{X}_m are drawn from the distribution $p(\mathbf{X})$. If P is very small, however, an unreasonable number of samples are necessary to produce events for which y is in Y_d , let alone enough to accurately approximate the integral. However, one can rewrite Eqs. (3.4a) and (3.4b) as follows:

$$\mathbb{P}[y \in Y_d] = \int I(y(\mathbf{x}))L(\mathbf{x})p_*(\mathbf{x})d\mathbf{x}, \quad (3.5a)$$

$$\hat{P}_{\text{ISMC}} = \frac{1}{M} \sum_{m=1}^M I(y(\mathbf{X}_{*,m}))L(\mathbf{X}_{*,m}), \quad (3.5b)$$

where the samples $\mathbf{X}_{*,m}$ are now drawn from the *biasing distribution* $p_*(\mathbf{X})$, and where the quantity $L(\mathbf{X}) = p(\mathbf{X})/p_*(\mathbf{X})$ is the *likelihood ratio*. When an appropriate biasing distribution is selected, importance-sampled Monte Carlo (ISMC) simulations can accurately estimate the probability of the sought-after rare events with a small fraction of the number of samples that would be necessary with straightforward MC methods. The challenge is, of course, to properly choose the biasing distribution. Indeed, in order for importance sampling to work, $p_*(\mathbf{X})$ should preferentially concentrate the MC samples around the *most likely* system realizations that lead to the rare events of interest. In our case the random variables \mathbf{X} are the noise components added at the end of each dispersion map period. Thus, in order to successfully apply IS we must find the most likely noise realizations that lead to a desired value of the soliton parameters at the output.

By substituting $\nu_n(x)$ into Eqs. (2.37a) and (2.37b) of Sec. II C, we immediately obtain the noise-induced parameter change at the n th map period as

$$\Delta Q_n = \frac{\text{Re} \int e^{-i\Theta(x)} \underline{y}_Q^*(x) \nu_n(x) dx}{\int \underline{y}_Q^*(x) y_Q(x) dx}, \quad (3.6)$$

where $Q=A, \Omega, X$ as before, with a slightly more complicated expression for $\Delta\Phi_n$. Moreover, for white Gaussian noise, maximizing the probability of a specific noise realization is equivalent to minimizing the negative of the argument of the exponential in the PDF, that is, minimizing the quantity

$$\int |\nu_n(x)|^2 dx. \quad (3.7)$$

Hence, in our case, the problem of determining the optimal biasing amounts to finding the noise realization that minimizes the integral in Eq. (3.7) subject to the constraint of achieving a desired parameter change, that is, subject to the constraint $\Delta Q_n = \Delta Q_{\text{target}}$, with ΔQ_n given by Eq. (3.6). This optimization problem can be solved by formulating Eqs. (3.7) and (3.6) as a Lagrange multiplier problem, as in Refs. [4,7]. Solving the resulting problem then yields $\nu_n(x) = \nu_{n,\text{opt}}(x)$, where

$$\nu_{n,\text{opt}}(x) = \frac{\text{Re} \int \underline{y}_Q^*(x') y_Q(x') dx'}{\int |\underline{y}_Q(x')|^2 dx'} \Delta Q_{\text{target}} e^{i\Theta(x)} \underline{y}_Q(x). \quad (3.8)$$

To induce a larger than normal parameter change, we then concentrate the MC samples around this optimal path. We do so by biasing the noise adding $\nu_{n,\text{opt}}(x)$ as a deterministic component; that is, we take

$$\nu_{*,n}(x) = \nu_{n,\text{opt}}(x) + \nu_n(x), \quad (3.9)$$

where $\nu_{n,\text{opt}}(x)$ is given by Eq. (3.8), and where $\nu_n(x)$ is also a white noise process satisfying Eqs. (3.3). [Recall that $\nu_n(x)$ and $\nu_n(x)$ are normalized noise processes, and the actual noise variance is ϵ^2 .]

Note that the optimal path $\nu_{n,\text{opt}}(x)$ depends on both the eigenmodes and the adjoint eigenmodes of the linearized DMNLS equation found in Sec. II. In particular, Eq. (3.8) implies that the optimal biasing is proportional to the *adjoint eigenmode* of the quantity that one desires to change, a result that might not be obvious *a priori*.

Once the most likely noise realization that produces a given parameter change ΔQ_n at each map period is known, one must also find the most likely way to distribute a total parameter change ΔQ_{tot} at the output among all map periods [5,7,18]. This further optimization problem can also be solved [18]. When targeting large amplitude or frequency changes, however, it suffices to simply distribute equally this total change among all map periods. That is, in the numerical simulations described in Sec. III B we set $\Delta Q_{\text{target}} = \Delta Q_{\text{tot}}/N_a$ for $n=1, \dots, N_a$. This is a good approximation as long as the variances of the noise-induced parameter change

at each amplifier are not too dissimilar. Such is indeed the case for amplitude and frequency in the ranges of values considered.

B. Importance-sampled Monte Carlo simulations

We now apply the ideas presented above to concrete numerical experiments of dispersion-managed systems under the effect of noise. We perform importance-sampled Monte Carlo (ISMC) simulations of the DMNLS equations (2.5a) and (2.5b) perturbed by noise, and we compare the results to standard Monte Carlo simulations of the original NLS equation with dispersion management (2.1), also subject to noise.

Let us discuss the approach we used for the numerical simulations of the noise-perturbed DMNLS equation. We simulate the evolution of a dispersion-managed optical signal by solving Eq. (2.5b) numerically and adding noise to the signal at periodically spaced time intervals. The initial condition, i.e., the input DMS shape at $t=0$, is generated by solving the nonlinear integral equation Eq. (2.10) as explained in Appendix 2, and time evolution is performed with a fast numerical method, as described in Appendix 1. White noise, which is added to the signal at $t=nt_a$ for $n=1, \dots, N_a$, is numerically discretized as a collection of independent, identically distributed zero-mean normal random variables, one each for the real and imaginary parts of the signal at each spatial grid point. Propagation and the addition of noise continue in this way until the signal reaches the output at $t_{\text{out}}=N_a t_a$.

In standard Monte Carlo simulations, one repeats the above process for several different noise realizations while monitoring the output value of the quantities of interest (e.g., energy and/or frequency), and then computes their statistics.

For importance-sampled Monte Carlo simulations, one also uses the basic framework described above. If one wants to obtain larger-than-normal deviations of a quantity Q , however, one also performs the following steps at each map period before adding the noise.

- (1) Recover the underlying DMS from the noisy signal. We do this by filtering the noisy pulse and using the resulting output, together with the numerically computed pulse parameters, as the initial condition in the iteration scheme for the nonlinear integral equation (A5). Further details are provided in Appendix 3.

- (2) Obtain the linear modes and adjoint modes of the linearized DMNLS equation around the given DMS. We do this by numerically calculating the x and s derivatives of the underlying DMS, and then using Eqs. (2.21a), (2.21b), (2.26a), and (2.26b). The x derivative is calculated using pseudospectral methods [34], while the derivative with respect to s is calculated by performing step (1) twice, once at the given value of s and once at $s+ds$.

- (3) Generate an unbiased noise realization, shift its mean with the appropriately scaled adjoint mode associated with Q according to Eqs. (3.9) and (3.8), and update the likelihood ratio.

One then adds the noise to the pulse, propagates the noisy signal to the next map period, and repeats this process until the signal reaches the output. For a given simulation, several

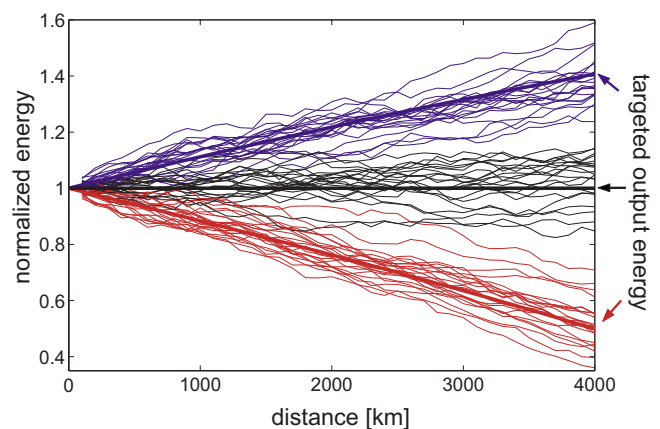


FIG. 3. (Color online) Samples from ISMC simulations of the DMNLS equation. Here, the pulse energy (normalized to input energy) is plotted as a function of time (i.e., distance in physical units). The arrows represent the different targeted output energies: A larger than normal output energy (blue), a smaller than normal output energy (red), and unbiased energy (black). Also plotted are deterministic paths (thick, smooth curves, with color corresponding to the target) predicted by our perturbation theory. These are the preferential paths around which we attempt to sample by biasing the noise with the adjoint linear modes. For each of three different targeted output energies, a few dozen ISMC samples are also shown (also colored correspondingly), demonstrating that the actual trajectories indeed follow the predictions of the theory. See text for a detailed discussion of system parameters.

thousand ISMC samples, generated with a few different biasing targets, are collected, and their contributions are combined using multiple importance sampling [9,35] in order to numerically generate the PDF of the quantity of interest.

Even though at each map period the noise induces only a small change in the solution parameters, these small changes can accumulate into large parameter changes at the output, resulting in a significantly distorted signal. This gradual build up of noise-induced distortions is evident in Fig. 3, where we plot the energy as a function of time for several different noise realizations biased around the optimal energy path predicted by the theory. For each sample path in this figure, the noise added at each map period is biased by adding a proper multiple of the adjoint amplitude mode in order to change the pulse amplitude and hence its energy. Note how the random samples are concentrated near the trajectories predicted by the theory. One can think of these trajectories as a low-dimensional projection of a near-optimal path through state space to reach a targeted rare event.

Note also that the linearized DMNLS equation is only used to guide the biasing, while, for each individual sample in the ISMC simulations, the full DMNLS equation is solved to propagate the signal. That is, no approximations are used for propagating the signal, and no assumptions are made about its shape to predict or calculate the pulse parameters at output. In other words, the only approximation in the simulations (beyond roundoff and truncation due to discretization) lies in using the information based on the linearized DMNLS equation in order to bias the noise. Thus, use of importance sampling enables full nonlinear simulation of large, noise-induced parameter changes.

C. Results and discussion

As a test of the method, we performed numerical simulations of two noise-perturbed dispersion-managed systems with different choices of system parameters. For both systems we compared ISMC simulations of the DMNLS equations (2.5a) and (2.5b) to standard MC simulations of the original NLS equation with dispersion management (2.1), numerically integrated with a standard second-order split-step Fourier method.

For both systems we chose the system parameters based on realistic values for optical fiber communication systems. Typical values of system parameters for the DMNLS as a model of femtosecond lasers can be obtained from Ref. [26]. In both cases we used a piecewise constant dispersion map. (That is, we considered the transmission link to be comprised of alternating sections of fiber with opposite signs of dispersion.) We used an average dispersion of $0.15 \text{ ps}^2/\text{km}$ a non-linear coefficient of 1.7 (W km)^{-1} , and a fiber loss of 0.21 dB/km . We set a unit time of 17 ps to define the normalized spacelike variable x in Eq. (2.1), and we used the resulting dispersion length of 1923 km to define the normalized time t , resulting in $\bar{d}=1$ in Eq. (2.1). We considered amplifiers spaced every 100 km (resulting in $t_a=0.052$), taking the dispersion map period to be aligned with the amplification period. The corresponding power needed to have $\bar{g}=1$ in Eq. (2.1) is 2.96 mW , and we used this value as a unit to normalize pulse powers.

For the first system, which we will refer to as system (a), we considered a map strength of $s=2$ and a propagation distance of 2000 km (resulting in $N_a=20$). For the second system, referred to hereafter as system (b), we considered a map strength of $s=4$ and a propagation distance of 4000 km (resulting in $N_a=40$). Thus, in both systems the average dispersion is small, while the local dispersion is large in magnitude. [Recall that the map strength parameter s quantifies the difference in magnitude between local and average values of dispersion, cf. Eq. (2.7).] For system (a) we used a DM soliton with $\lambda=1.5$ as initial condition (corresponding to an initial pulse with 6.66 mW peak power) and for system (b) we took $\lambda=2$ (corresponding to 11.8 mW). Assuming a spontaneous emission factor of 1.5 , system (a) has an optical signal-to-noise ratio of 16.7 (resulting in a dimensionless noise variance $\epsilon^2=2.372 \times 10^{-4}$) and system (b) of 13.8 (resulting in $\epsilon^2=9.486 \times 10^{-4}$).

In system (a) we looked for large changes in frequency at the output. In system (b) we looked for large changes in amplitude and hence in output energy. The output distributions of both frequency and energy are of course of practical interest in communications, since large deviations of each quantity will result in transmission errors. Frequency changes translate in group velocity changes, and hence in the pulse walking off its assigned bit slot. Similarly, a pulse that loses a significant fraction of its energy will be incorrectly detected in an amplitude-shift-keyed system.

In Fig. 4 we plot the PDF of the output frequency of pulses from the dispersion-managed system (a) described above. We performed standard MC simulations of the noise-perturbed NLS equation with DM (2.29), with $100\,000$ samples to estimate the PDF of output frequency (red dots).

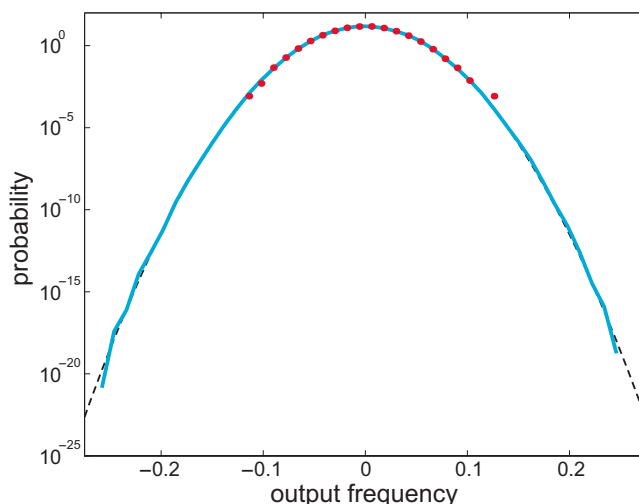


FIG. 4. (Color online) PDF of output frequency in a dispersion-managed system. The solid (cyan) curve shows results from ISMC simulations of the DMNLS Eq. (2.5) with $75\,000$ samples. The (red) dots are the results from standard MC simulations of the NLS equation with DM, Eq. (2.1) with $100\,000$ samples. The (black) dashed curve is a Gaussian PDF obtained from Gordon-Haus theory of the NLS equation with DM. Note how unbiased MC simulations of the NLS equation with DM agree with the ISMC simulation of the DMNLS and the Gaussian distribution to that simulation as far down in probability as the unbiased simulations can reach.

We also plot a Gaussian PDF (black dashed line) whose variance is consistent with a theoretical model of Gordon-Haus effect for a DM system governed by the noise-perturbed NLS equation in the presence of dispersion management (2.29) [37,38,36], assuming a Gaussian ansatz for the pulse shape at the chirp-free point. Finally, we performed ISMC simulations of the noise-perturbed DMNLS equation (2.30) with $75\,000$ samples, and we plot the corresponding results for the PDF of output frequency (cyan solid line). The results of ISMC simulations of the DMNLS equation, of standard MC simulations of the NLS equation with DM, and the Gaussian fit to that simulation all match exactly to very small probabilities. This comparison demonstrates the effectiveness of using the modes of the linearized DMNLS equation to find rare events in dispersion-managed optical systems.

In Fig. 5 we plot the PDF of the output energy of pulses in dispersion-managed system (b) described above. Here, as in Fig. 3, energy is normalized by the energy of the input signal, i.e., by the “back-to-back” signal energy. Again, the red dots show results of standard MC numerical simulations of the noise-perturbed NLS equation with DM, with $1\,000\,000$ samples; the black dashed line shows a Gaussian fit to the results of these simulations, and the cyan solid line shows the results of ISMC simulations of the noise-perturbed DMNLS equation, with $42\,000$ samples. It is worth noting that the PDF generated from standard MC simulations of the NLS equation with DM clearly deviates from the Gaussian fit, but it agrees very well with the ISMC simulations of the DMNLS equation, as far down in probability as the unbiased MC simulations can reach. These comparison provides a strong validation of the DMNLS equation as a model of dispersion-managed lightwave systems.

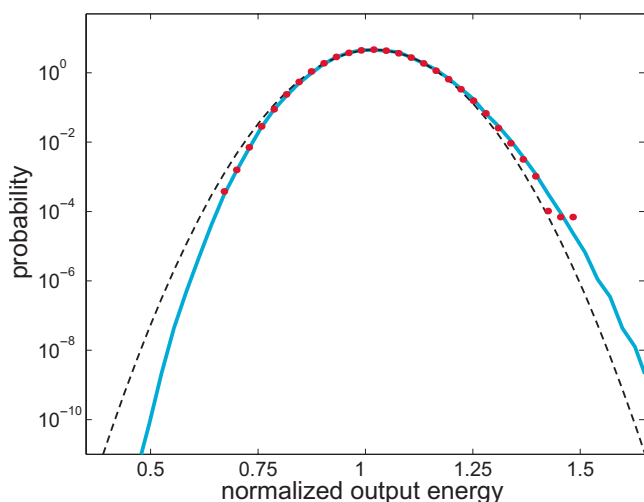


FIG. 5. (Color online) PDF of normalized output energy. The solid (cyan) curve shows results from ISMC simulations of the DMNLS with 42 000 samples. The (red) dots are the results from standard MC simulations of the NLS equation with DM with 1 000 000 samples. The (black) dashed curve is a Gaussian fit to that simulation. Note how unbiased MC simulations of the NLS equation with DM clearly deviate from Gaussian, but agree well with ISMC simulations of the DMNLS as far down in probability as the unbiased simulations can accurately reach.

IV. CONCLUSIONS

We have described a perturbation theory for soliton-based dispersion-managed lightwave systems, whose dynamics is governed by the dispersion-managed NLS (DMNLS) equation, and we used the results of the theory to guide importance-sampled Monte Carlo simulations to quantify the effects of noise in these systems. The present theory differs from the soliton perturbation theory that applies to the NLS equation in several important respects. First, due to the loss of integrability, the eigenmodes of the linearized DMNLS equation are derived from the invariances of the equation rather than from the inverse scattering method. Second, the DMNLS equation is not scale-invariant, but is invariant under a generalized scaling transformation; as a consequence the amplitude mode depends explicitly on the map strength. Third, unlike for the NLS equation, the linear modes of the DMNLS equation are not automatically normalized, and in particular their norms and inner products depend on both the map strength and the pulse energy.

The results of importance-sampled numerical simulations of the noise-perturbed DMNLS equations agree very well with the results of Gordon-Haus theory for dispersion-managed systems (which are based on the original NLS equation) as well with the results of standard Monte Carlo simulations of the original NLS equation with dispersion management as far down as those can go in probability. This is true even when those results deviate from Gaussian distributions. Both of these results provide a further important test of the validity of the DMNLS equation as a model of dispersion-managed lightwave systems.

It should be noted that, in some parameter regimes, the DMNLS equation also admits internal modes [21] (see also

Refs. [19,25]). In principle, the accumulation of noise into such internal modes could also contribute to system failures. If no generalized modes are associated with these modes, however, the variance of the resulting noise-induced pulse fluctuations will grow linearly in time, as opposed to cubically (as is the case for phase and timing fluctuations). Therefore, over long distances (that is, for systems in which the total propagation distance is much larger than the average dispersion length), one would expect these modes not to be the dominant source of errors. Such is the case for transmission links over transoceanic distances and for femtosecond lasers. The situation might be different over shorter distances. In that case, one should be able to estimate the contribution of the internal modes using a suitably generalized version of the perturbation theory described here. Of course, these arguments must be validated by more precise calculations and/or careful numerical experiments.

ACKNOWLEDGMENTS

It is a pleasure to thank M. J. Ablowitz, W. L. Kath, and C. R. Menyuk for many interesting discussions. This work was supported by the National Science Foundation under Grant No. DMS-0506101.

APPENDIX: NUMERICAL METHODS FOR THE DMNLS EQUATION

Here we discuss numerical methods for the DMNLS equation (2.5a), which were used in our numerical simulations. We address three issues: (i) Numerical methods for time integration; (ii) numerical methods to find traveling-wave solutions; and (iii) numerical methods to extract a dispersion-managed soliton from the noisy signal.

1. Time integration of the DMNLS equation

We first discuss time integration methods for the DMNLS equation. Equation (2.5a) differs from a PDE because of the double integral, and it should be obvious that the most computationally expensive task when trying to integrate it numerically is the evaluation of the double integral in either of Eqs. (2.5a) and (2.5b). If N_x is the number of grid points in x (or ω), a straightforward quadrature scheme requires $O(N_x^3)$ operations (since one needs to evaluate a different double integral for each value of x or ω). As we now show, however, it is possible to evaluate the integral with only $O(JN_x \log N_x)$ operations, where J is an integer parameter whose meaning will become clear shortly.

Let us denote the double integral in Eq. (2.5b) as

$$\hat{K}(\omega, t) = \int \int \hat{u}'_{(\omega+\omega')} \hat{u}'_{(\omega+\omega'')} \hat{u}'_{(\omega+\omega'+\omega'')} r_{(\omega' \omega'')} d\omega' d\omega'' \quad (\text{A1})$$

(where we reinstated the primes to distinguish the solution of the DMNLS equation from that of the original NLS problem). Recall from Eq. (2.3) that $\hat{u}(\omega, t, \zeta) = \hat{u}'(\omega, t) e^{-iC(\zeta)\omega^2/2}$ is the leading-order solution of the original NLS equation

with dispersion management, namely Eq. (2.1). Also recall from Eq. (2.6a) that the kernel $r(x)$ is an average over a dispersion map period, and $R(t, t') = \mathcal{F}_{t, t'}^{-1}[r(\omega\omega')]$. Indeed, retracing backwards the steps of the multiple scale expansion used to obtain the DMNLS equation [11], one can express the whole quantity $\hat{K}(\omega, t)$ as an average:

$$\hat{K}(\omega, t) = \int_0^1 e^{iC(\zeta)\omega^2/2} g(\zeta) \mathcal{F}_\omega[(|u|^2 u)(x, t, \zeta)] d\zeta, \quad (\text{A2})$$

where $u(x, t, \zeta) = \mathcal{F}_t^{-1}[\hat{u}(\omega, t, \zeta)]$. Note that t is a constant in the integral on the RHS of Eq. (A2), and this is precisely the key for the fast numerical computation of $\hat{K}(\omega, t)$.

Divide the interval $[0, 1]$ into J equally spaced points ζ_0, \dots, ζ_J , with $\zeta_0 = 0$ and $\zeta_J = 1$. For each fixed value of t we can calculate $\hat{K}(\omega, t)$ as follows.

- (1) Fix ζ_j and construct $\hat{u}(\omega, t, \zeta_j) = \hat{u}'(\omega, t) e^{-iC(\zeta_j)\omega^2/2}$.
- (2) Take the inverse Fourier transform to obtain $u(x, t, \zeta_j)$ and construct the product $|u|^2 u$.
- (3) Take the direct Fourier transform to obtain $\mathcal{F}_\omega[|u|^2 u]$.
- (4) Multiply the result by $g(\zeta_j) e^{iC(\zeta_j)\omega^2/2}$ to obtain the integrand in Eq. (A2).
- (5) Repeat steps (1)–(4) for all grid points ζ_j and evaluate the integral in Eq. (A2) to obtain $\hat{K}(\omega, t)$.

The DMNLS equation can now be integrated in time using any desired numerical scheme. For example, one can use an exact integrating factor on the linear part of Eqs. (2.5a) and (2.5b) and an explicit fourth-order Runge–Kutta method for the nonlinear part. A few remarks are now in order.

The above procedure, which can be carried out for any choice of dispersion map and nonlinear coefficient, is a generalization of an algorithm originally introduced in Ref. [23] and it is essentially the same as that described in Ref. [24] for the NLS equation, except that no approximations are necessary here. Indeed, the method of Ref. [24] parallelizes the numerical solution of the NLS equation precisely by approximating it with the DMNLS equation.

Steps (2) and (3) each cost $O(N_x \log N_x)$ operations. Since they must be repeated for each of the grid points ζ_0, \dots, ζ_J , the overall complexity of the algorithm is $O(JN_x \log N_x)$.

In essence, the algorithm reduces the calculation of $\hat{K}(\omega, t)$ to that of the effective nonlinearity in the original NLS equation, averaged over one period of the dispersion map.

In practice, the value of J is dictated by the value of the map strength and the need to adequately resolve the changes in the integrated dispersion function $C(\zeta)$. The same requirements however also dictates the integration step size in the original NLS problem. The computational complexity of the DMNLS equation (2.5a) is thus the same as that of the original NLS problem (2.1).

It appears more advantageous to integrate Eq. (2.5b) rather than Eq. (2.5a), since this allows one to treat the linear (stiff) portion of the PDE exactly. Also, the use of a split-step method does not seem as desirable here (unlike the case of the NLS equation), since it is not possible to integrate the nonlinear portion exactly.

2. Traveling-wave solutions of the DMNLS equation

We now discuss a numerical method to find stationary solutions of the DMNLS equation, i.e., dispersion-managed solitons (DMS). That is, we look for solutions of Eq. (2.5a) in the form

$$u'_{\text{st}}(x, t) = f(x) e^{i\lambda^2 t/2}, \quad (\text{A3a})$$

or, equivalently, solutions of Eq. (2.5b) in the form

$$\hat{u}'_{\text{st}}(\omega, t) = \hat{f}(\omega) e^{i\lambda^2 t/2}. \quad (\text{A3b})$$

Once such a stationary solution is available, a three-parameter family of traveling waves can be generated using the translation, phase, and Galilean invariance of the DMNLS equation. That is, if $u'_{\text{st}}(x, t)$ is any solution of Eq. (2.5a), so is

$$u'_{\Omega, x_o, \phi_o}(x, t) = e^{i[\Omega x - \bar{d}\Omega^2 t/2 + \phi_o]} u'_{\text{st}}(x - x_o - \bar{d}\Omega t, t), \quad (\text{A4})$$

where Ω , x_o , and ϕ are arbitrary real parameters.

Inserting Eq. (A3b) into the DMNLS equation yields the nonlinear integral equation (2.10), which we rewrite here for convenience:

$$\hat{f}(\omega) = \frac{2}{\lambda^2 + \bar{d}\omega^2} \int \int \hat{f}(\omega+\omega') \hat{f}(\omega+\omega'') \hat{f}^*(\omega+\omega'+\omega'') r(\omega'\omega'') d\omega' d\omega''. \quad (\text{A5})$$

For each fixed value of λ , Eq. (A5) yields the shape of the corresponding dispersion-managed soliton. (Or, rather, its Fourier transform.) Thus, for each value of s , λ plays the role of a nonlinear eigenvalue, which is in one-to-one correspondence with the dispersion-managed soliton's energy. For the NLS equation, one simply has $u(x, t) = A \operatorname{sech}[Ax] e^{iA^2 t/2}$; thus $\lambda = A$ is exactly half of the pulse energy: $\int |u_s(x, t)|^2 dx = 2A$. This is related to the existence of a simple scaling invariance: If $u_o(x, t)$ is any solution of NLS, so is $u(x, t) = \lambda u_o(\lambda x, \lambda^2 t)$. When the map strength is nonzero, however, this invariance is lost, and the scaling invariance of the DMNLS equation is more complicated than that of the NLS equation, as discussed in Sec. II. As a consequence, a different integral equation (A5) must be solved to obtain the soliton shape for each given value of λ , unlike the NLS equation.

A first approach to solving Eq. (A5) is to apply a Neumann iteration scheme: $\hat{f}_{(\omega)}^{(n+1)} = R[\hat{f}_{(\omega)}^{(n)}]$ [39], where $R[\hat{f}_{(\omega)}]$ denotes the right-hand side of Eq. (A5). Such an iteration scheme is divergent, however. The key is to apply a modified iteration scheme:

$$\hat{f}_{(\omega)}^{(n+1)} = C^\alpha[\hat{f}_{(\omega)}^{(n)}] R[\hat{f}_{(\omega)}^{(n)}], \quad (\text{A6})$$

where the convergence factor $C[\hat{f}]$ is

$$C[\hat{f}] = |s_L[\hat{f}]/s_R[\hat{f}]|, \quad (\text{A7a})$$

with

$$s_L[\hat{f}] = \int |\hat{f}(\omega)|^2 d\omega, \quad s_R[\hat{f}] = \int \hat{f}^*(\omega) R[\hat{f}(\omega)] d\omega. \quad (\text{A7b})$$

Again, a few remarks.

The method discussed in Appendix 1 for the computation of the double integral in the DMNLS equation also applies, of course, for the calculation of the double integral in Eq. (A5).

Since $C[\hat{f}] = 1$ for all solutions $\hat{f}(\omega)$ of Eq. (A5), any solution of Eq. (A5) is also a solution of the modified integral equation $\hat{f}(\omega) = C^\alpha[\hat{f}]R[\hat{f}(\omega)]$, for which Eq. (A6) is a standard Neumann iteration scheme.

Since $C[\hat{f}] = 1$ when $\hat{f}(\omega)$ is a solution of Eq. (A5), the value of $C[\hat{f}]$ can be used as a monitor of convergence, for example by requiring that $|1 - C[\hat{f}]|$ drop below a predefined threshold (e.g., 10^{-12} or 10^{-16}) as a termination condition.

This iteration scheme, which was first used in Ref. [11] to find the shape of dispersion-managed solitons, is based on a method introduced in Ref. [40]. A proof of the convergence of this method for evolution equations with power-law nonlinearity was recently given in Ref. [41].

As might be expected, the choice of α is crucial. Indeed, it can be shown that the method converges for $1 < \alpha < 2$, and optimal convergence is obtained for $\alpha = \frac{3}{2}$. Note, however, that $\bar{d} \geq 0$ is required for convergence. When $\bar{d} < 0$, the denominator of the RHS of Eq. (A5) has two simple poles at $\omega = \pm \lambda / |\bar{d}|^{1/2}$, and even the modified iteration diverges. A method to obtain solutions with $\bar{d} < 0$ was used in [25]; that method, however, was later shown to be divergent [23].

3. Extraction of a DM soliton from a noisy signal

Finally, we now describe the algorithm we used to extract the underlying DM soliton from a noisy signal. This section expands on the brief comments given in Sec. III B.

To perform soliton extraction, one first needs to identify the relationship between the energy E and pulse amplitude λ . Unlike the case of the NLS equation, no closed-form relation is known between these two parameters. This relationship, however, can be numerically “precomputed” and recorded for later use as follows. First one chooses a fine, uniform grid of values of λ over a sufficiently large range of values (in our case, $[0.5, 3]$). Then, for each fixed value of map strength s ,

one solves Eq. (A5) for each value of λ to find the Fourier transform $\hat{f}(\omega)$ of the corresponding pulse shape $f(x)$. The energy E of each computed pulse shape is simply given by $E = \int |f(x)|^2 dx$. Note that, since $y_{\bar{A}} = iu$ up to a phase, this is exactly the method that was used to produce the curves of $\|y_{\bar{A}}\|$ as a function of λ in Fig. 2.

Now, suppose we have a noisy pulse that has propagated to the n th amplifier. The extraction of the DM soliton at $t = nt_a^-$ from $u(x, nt_a^-)$ proceeds as follows.

(1) Obtain a first approximation to the soliton frequency Ω by computing the mean frequency of the noisy pulse

$$\Omega_o = \int \omega |\hat{u}(\omega, nt_a^-)|^2 d\omega / \int |\hat{u}(\omega, nt_a^-)|^2 d\omega, \quad (\text{A8})$$

where as before $\hat{u}(\omega, t)$ is the Fourier transform of $u(x, t)$.

(2) Filter the noisy pulse. We do so using a low-pass Gaussian filter centered at Ω_o . That is, we define

$$\hat{u}_f(\omega) = \hat{u}(\omega, t) \exp[-(\omega - \Omega_o)^2 / 2\Delta\Omega_f^2], \quad (\text{A9})$$

where the subscript f denotes the filtered pulse and where $\Delta\Omega_f$ is some appropriate low-pass filter width.

(3) Refine the approximation on the frequency parameter Ω by replacing $\hat{u}(\omega, nt_a^-)$ with the filtered pulse $\hat{u}_f(\omega)$ in Eq. (A8).

(4) Approximate the DM soliton parameter λ by calculating the energy of the filtered pulse, $E = \int |u_f(x)|^2 dx$, and finding the value of λ that corresponds to this energy in the precomputed table (interpolating between values if needed).

(5) Plug the estimated values for the parameters λ and Ω into Eq. (A5) and use the filtered pulse $\hat{u}_f(\omega, nt_a^-)$ as initial condition to find the underlying DM soliton using the method described in Appendix 2. Note that when Ω is non-zero we replace the denominator in Eq. (A5) with $\lambda^2 + \bar{d}(\omega - \Omega)^2$, so as to automatically obtain a DMS shape with the correct carrier frequency.

Note that, unless one wants to calculate phase or position parameters for the purpose of collecting statistics, there is no need to estimate those parameters, because the linear modes are found by taking (numerical) derivatives of the DM soliton found in step (5).

We also emphasize that the above approximations only affect how the noise is biased, and do not have any effect on pulse propagation. That is, no approximations are made when computing the signal evolution.

-
- [1] G. P. Agrawal, *Nonlinear Fiber Optics* (Academic Press, San Diego, 2001).
 [2] L. F. Mollenauer and J. P. Gordon, *Solitons in Optical Fibers: Fundamentals and Applications* (Academic Press, New York, 2006).
 [3] *Femtosecond Optical Frequency Comb: Principle, Operation and Applications*, edited by J. Ye and S. T. Cundiff (Springer, New York, 2004).
 [4] R. O. Moore, G. Biondini, and W. L. Kath, *Opt. Lett.* **28**, 105

- (2003).
 [5] R. O. Moore, G. Biondini, and W. L. Kath, *SIAM J. Appl. Math.* (to be published 2007).
 [6] R. O. Moore, T. Schafer, and C. K. R. T. Jones, *Opt. Commun.* **256**, 439 (2005).
 [7] E. Spiller, W. Kath, R. Moore, and C. McKinstrie, *IEEE Photonics Technol. Lett.* **17**, 1022 (2005).
 [8] A. Tonello, S. Wabnitz, I. Gabitov, and R. Indik, *IEEE Photonics Technol. Lett.* **18**, 886 (2006).

- [9] G. Biondini, W. L. Kath, and C. R. Menyuk, *IEEE J. Lightwave Technol.* **22**, 1201 (2004); **24**, 1065 (2006).
- [10] R. Srinivasan, *Importance Sampling: Applications in Communications and Detection* (Springer, Berlin, 2002).
- [11] M. J. Ablowitz and G. Biondini, *Opt. Lett.* **23**, 1668 (1998).
- [12] M. J. Ablowitz, B. Ilan, and S. T. Cundiff, *Opt. Lett.* **29**, 1808 (2004).
- [13] I. R. Gabitov and S. K. Turitsyn, *Opt. Lett.* **21**, 327 (1996).
- [14] M. J. Ablowitz, G. Biondini, and T. Hirooka, *Opt. Lett.* **26**, 459–461 (2001).
- [15] M. J. Ablowitz, G. Biondini, and E. S. Olson, *J. Opt. Soc. Am. B* **18**, 577 (2001).
- [16] M. J. Ablowitz, T. Hirooka, and T. Inoue, *J. Opt. Soc. Am. B* **19**, 2876 (2002).
- [17] G. Biondini and S. Chakravarty, *Opt. Lett.* **26**, 1761 (2001).
- [18] G. Biondini, W. L. Kath, J. Li, and E. Spiller (unpublished).
- [19] A. D. Capobianco, G. Nalesso, A. Tonello, F. Consolandi, and C. De Angelis, *Opt. Lett.* **28**, 1754 (2003).
- [20] T. I. Lakoba, *Phys. Lett. A* **260**, 68 (1999).
- [21] T. I. Lakoba and D. E. Pelinovsky, *Chaos* **10**, 539 (2000).
- [22] P. M. Lushnikov, *Opt. Lett.* **25**, 1144 (2000).
- [23] P. M. Lushnikov, *Opt. Lett.* **26**, 1535 (2001).
- [24] P. M. Lushnikov, *Opt. Lett.* **27**, 939 (2002).
- [25] D. E. Pelinovsky, *Phys. Rev. E* **62**, 4283 (2000).
- [26] Q. Quraishi, S. T. Cundiff, B. Ilan, and M. J. Ablowitz, *Phys. Rev. Lett.* **94**, 243904 (2005).
- [27] A. Tonello, A. D. Capobianco, and G. Nalesso, *Opt. Commun.* **246**, 15 (2005).
- [28] A. Tonello, A. D. Capobianco, G. Nalesso, F. Gringoli, and C. De Angelis, *Opt. Commun.* **246**, 393 (2005).
- [29] J. D. Ania-Castanon, T. J. Ellingham, R. Ibbotson, X. Chen, L. Zhang, and S. K. Turitsyn, *Phys. Rev. Lett.* **96**, 023902 (2006).
- [30] D. J. Kaup, *Phys. Rev. A* **42**, 5689 (1991).
- [31] A. Hasegawa and Y. Kodama, *Solitons in Optical Communications* (Oxford University Press, Oxford, 1995).
- [32] C. M. Bender and S. A. Orszag, *Advanced Mathematical Methods for Scientists and Engineers* (Springer, Berlin, 1999).
- [33] E. Iannone, F. Matera, A. Mecozzi, and M. Settembre, *Nonlinear Optical Communication Networks* (Wiley, New York, 1998).
- [34] B. Fornberg, *A Practical Guide to Pseudospectral Methods* (Cambridge University Press, Cambridge, UK, 1998).
- [35] E. Veach, Ph.D. thesis, Stanford University, 1997 (unpublished).
- [36] N. J. Smith, W. Forsyiaik, and N. J. Doran, *Electron. Lett.* **32**, 2085 (1996).
- [37] S. Kumar and F. Lederer, *Opt. Lett.* **22**, 1870 (1998).
- [38] C. J. McKinstrie, *Opt. Commun.* **200**, 165 (2001).
- [39] L. M. Delves and J. L. Mohamed, *Computational Methods for Integral Equations* (Cambridge University Press, Cambridge, UK, 1985).
- [40] V. I. Petviashvili, *J. Plasma Phys.* **2**, 257 (1976).
- [41] D. E. Pelinovsky and Y. A. Stepanyants, *SIAM (Soc. Ind. Appl. Math.) J. Numer. Anal.* **42**, 1110 (2004).